

# Two Photon Physics at a Future Linear Collider<sup>†</sup>

Richard Nisius

*CERN,*

*CH-1211 Genève 23, Switzerland*

*E-mail: Richard.Nisius@cern.ch*

## Abstract

Some general considerations on a future linear collider and selected topics of two photon physics measurements which can be performed at such a collider are presented. This review discusses the total photon-photon cross section, jet cross sections, structure functions, charm production, the BFKL Pomeron,  $W$  pair production, and Higgs production.

---

## 1 Introduction

With the advent of a future linear collider two photon physics will be important for several reasons. Firstly the high centre-of-mass energy in the order of 0.5–2 TeV enables to extend the two photon physics measurements performed at LEP. Examples of such measurements are the measurements of the photon structure functions which can be performed at much higher momentum transfer squared of the virtual photon and the measurements of the total photon-photon cross section and of jet cross sections in photon-photon scattering which can be extended to larger invariant masses and jet transverse momenta. Secondly two photon physics gets extended to new channels, especially if a photon linear collider, PLC, can be build [1]. In such a case the linear collider will be a  $W$ -factory with millions of polarised  $W$  pairs being produced per year. Even more important will be the fact that the Higgs boson can be produced in the photon-photon fusion process  $\gamma\gamma \rightarrow H$ . The study of this process will provide very valuable information on how particle masses are generated. Thirdly two photon physics processes will play an even more important role as background for searches for new physics than they already do in searches performed at LEP. The material presented here is a personal collection of topics which I find interesting and it is not a complete survey of all topics under study. The review mainly relies on the work done within the DESY ECFA study groups on the physics potential of a future linear collider.

---

<sup>†</sup>Invited talk at the Workshop on photon interactions and the photon structure, 10-13 September 1998, Lund, Sweden, to appear in the Proceedings.

## 2 The Instruments

There are several research programmes around the world which investigate different options on how to build a future linear collider. The individual projects pursued today are, CLIC [2], JLC [3], NLC [4] and TESLA [5]. This review only discusses the physics measurements which can be performed at such a collider and it does not consider the arguments in favour or against the individual attempts and also not the prospects for the construction of a PLC. Only the general features of a generic linear collider, see Figure 1 for a sketch, are addressed below. The linear collider is an extension of the existing  $e^+e^-$

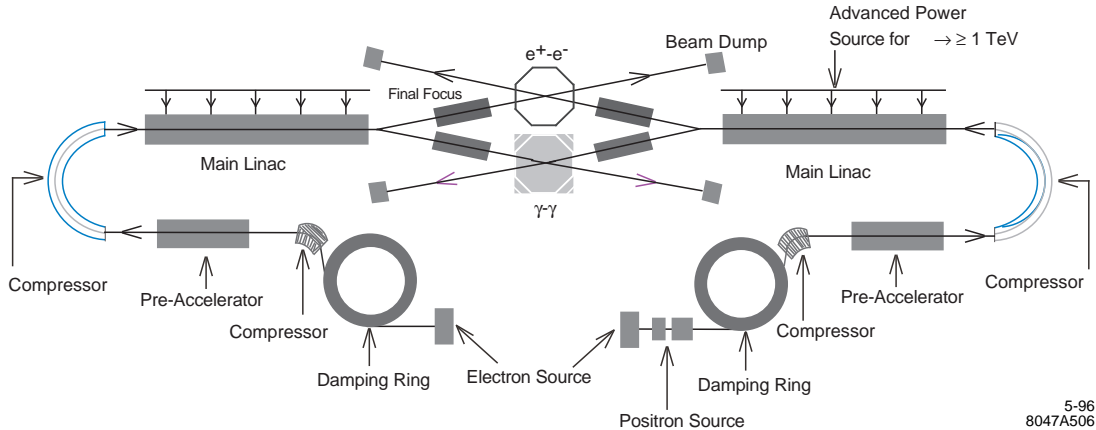


Figure 1: The general layout of a future linear collider, from Ref. [4].

colliders LEP and SLC. Table 1 shows the improvements on several machine parameters which have to be achieved in order to arrive at a luminosity of the order of  $10^{34}/\text{cm}^2\text{s}$ , which would lead to an integrated luminosity of about  $100 \text{ fb}^{-1}$  per year of operation.

	LEP	SLC	TESLA
total length [km]	26.7	4	33
gradient [MV/m]	6	10	25
beam size $\sigma_x/\sigma_y$ [ $\mu\text{m}/\mu\text{m}$ ]	110 / 5	1.4 / 0.5	0.845/0.019
electron energy [GeV]	100	50	250
luminosity [ $10^{31}/\text{cm}^2\text{s}$ ]	7.4	0.1	5000-10000
$\mathcal{L}_{int}$ [1/pb y]	200	15	20000

Table 1: Some approximate values of parameters of the present LEP and SLC colliders and goals for a future linear collider of the TESLA design.

For several reactions the cross sections for incoming photons are larger than for incoming electrons of the same energy, see Section 3, and some reactions like e.g. the very important process  $\gamma\gamma \rightarrow H$  are only possible in reactions of high energetic photons. Therefore there is a strong interest in the construction of a PLC, which would be an ideal source of high energetic photons. In order to build a PLC several constrains have to be imposed on the machine and the interaction region of a  $\gamma\gamma$  collider, shown schematically in Figure 1, has to be designed differently than an interaction region for the  $e^+e^-$  collider. The general procedure to produce a beam of high energetic photons from the electron beam by means of the Compton backscattering process is shown in Figure 2.

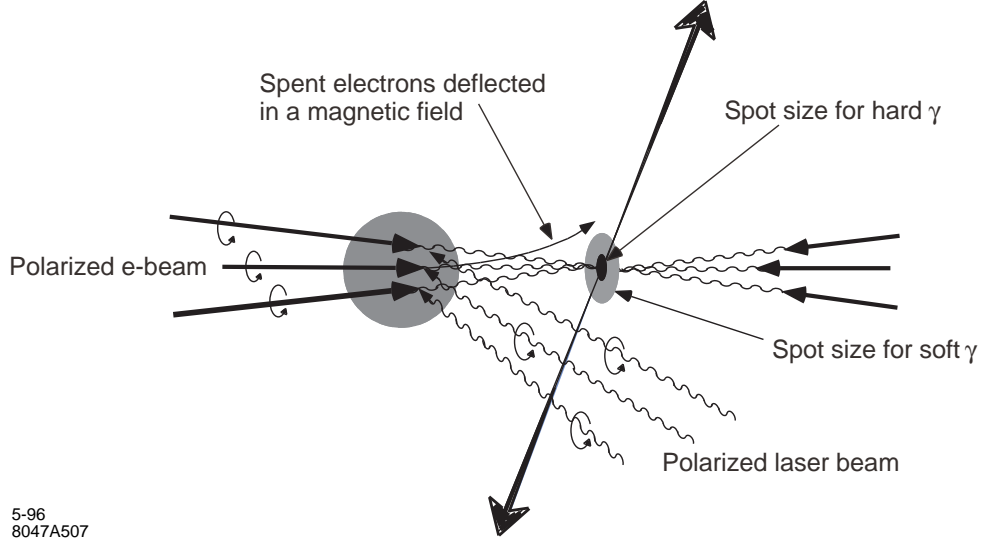


Figure 2: A sketch of the creation of the photon beam by Compton backscattering of laser photons off the beam electrons, from Ref. [4].

The photons are produced by a high intensity laser and brought into collision with the electron beams at distances of about 0.1–1 cm from the interaction point. The photons are scattered into a small cone around the initial electron direction and receive a large fraction of the electron energy. The opening angle is such that the high energetic photons produce a smaller beam spot than the softer ones. If the Compton scattering is done on one side (two sides) than the collider runs in the  $e\gamma$  ( $\gamma\gamma$  mode). For a  $\gamma\gamma$  collider there will always be remaining  $e\gamma$  and  $ee$  luminosities, Figure 3(a), because some of the leftover electrons of the so called spent beams will reach the interaction region. The remaining  $e\gamma$  and  $ee$  luminosities can considerably be reduced by magnetic deflection of the spent beam, Figure 3(b).

The critical parameters of a PLC are the achievable  $\gamma\gamma$  luminosity, the energy spectrum of the Compton scattered photons, the resulting polarisation of the photon beam, the background produced at the interaction region, and the remaining  $e\gamma$  and  $ee$  luminosities. Within limits several of these parameters can be chosen at will [6, 7] by changing the distance along the beam line between of the production of the backscattered photons and the interaction region,  $b$ , by selecting the polarisation of the laser beam,  $P_c$ , and the polarisation of electron beam,  $\lambda_e$ , and by magnetic reflection of the spent beam, as illustrated in Figure 3(c,d). The most peaked energy distribution is achieved for  $2P_c\lambda_e = -1$  and  $b \rightarrow 0$ . Here  $k = N_\gamma/N_e$  is the fraction of electrons that can be converted into photons and  $a$  is the r.m.s radius of the electron beam at the interaction point. The symbols  $\omega_0$  and  $E_0$  denote the energies of the laser photons and beam electrons, respectively and  $x = \frac{E_0\omega_0}{m^2c^4}$ , with  $m$  being the mass of the electron. The geometrical luminosity,  $L_{ee} = L_{\text{geom}}$ , is defined as  $L_{\text{geom}} = N^2 f / (4\pi\sigma_x\sigma_y)$ , where  $N$  is the number of particles in the beam,  $f$  is the repetition frequency, and  $\sigma_x$  and  $\sigma_y$  are the transverse beam sizes at the interaction point. In summary a typical distribution of  $\gamma\gamma$  and  $e\gamma$  luminosity as a function of the invariant mass peaks at the maximum reachable invariant mass of around  $0.8\sqrt{s_{ee}}$  with widths of  $\Delta W_{\gamma\gamma}/W_{\gamma\gamma} \approx 0.15$  for  $\gamma\gamma$ , and  $\Delta W_{e\gamma}/W_{e\gamma} \approx 0.05$  for  $e\gamma$  collisions [7].

The linear collider, even when running in optimal conditions will produce a huge

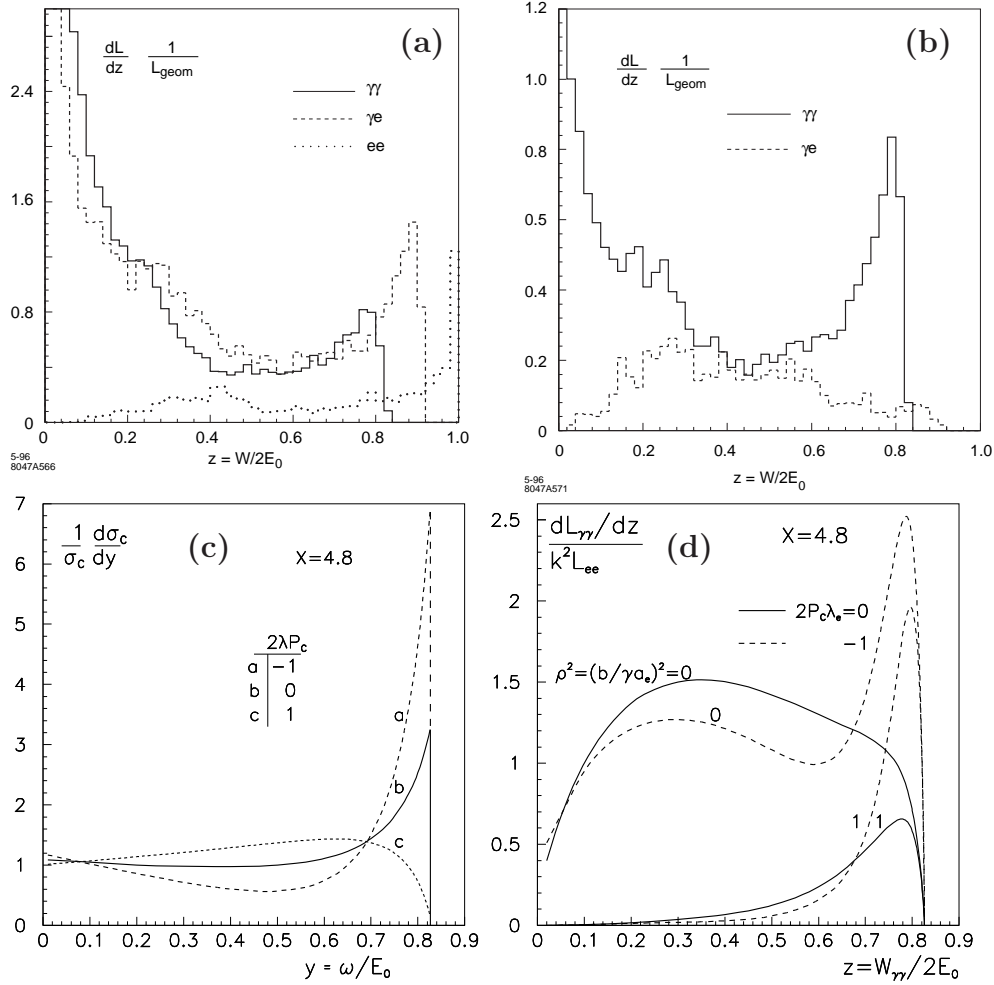


Figure 3: Some expected distributions for critical parameters of a PLC, from Ref. [4, 6]. Shown are (a) the luminosity spectrum without deflection of the spent beam for a vertical offset of the beam of  $0.75\sigma_y$  and a distance of  $b = 0.5$  cm, (b) the luminosity spectrum with deflection of the spent beam with  $B = 1$  T and a distance of  $b = 0.78$  cm, (c) the energy spectrum of the Compton scattered photons for fixed  $x$  and different polarisations of the laser photons and the beam electrons as a function of the photon energy divided by the energy of the beam electrons, and (d) the luminosity spectrum as a function of the photon-photon centre-of-mass energy scaled by the  $e^+e^-$  centre-of-mass energy for different polarisations and distances between the conversion point and the interaction point.

amount of background where many particles are produced especially in the forward regions of the detector. In order to cope with this background the detector has to be shielded with a massive mask as shown e.g. for the TESLA design in Figure 4.

Detailed background studies for the linear collider were performed. The background sources are synchrotron radiation in the last doublet of quadrupole magnets and the final focus system, muons accompanying the beams, beamstrahlung (photon radiation of electrons of one beam in the strong field of the electrons of the other beam) which will mainly lead to  $e^+e^-$  pair creation, hadronic background and for a PLC also losses of the spent beams. The photon radiation will lead to a significant energy smearing for the

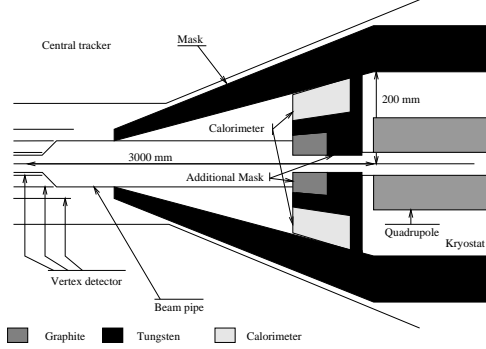


Figure 4: A sketch of the proposed mask for the TESLA design to protect the detector from the background, from Ref. [8].

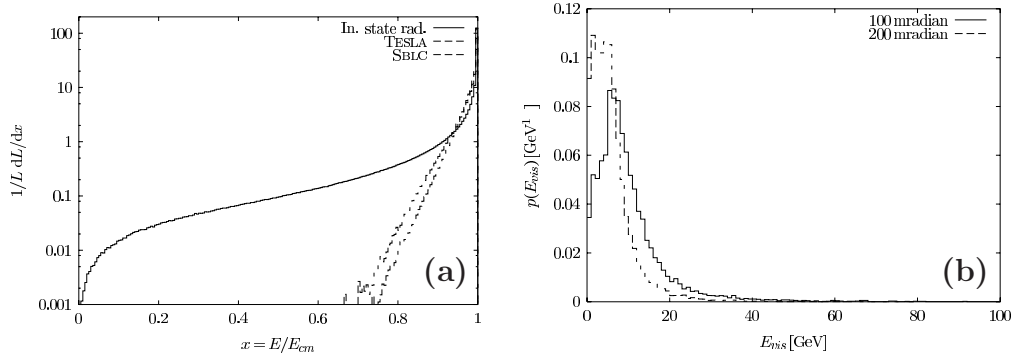


Figure 5: Some features of the expected background, from Ref. [8]. Shown are (a) the luminosity spectrum at the interaction point as a function of the electron energy scaled by the nominal energy of the beam electrons, where the energy losses shown are due to initial state radiation and beamstrahlung and (b) the distribution of the visible energy of hadronic events for two different acceptance boundaries for the detection of hadrons of 100 mrad and 200 mrad.

electrons of the beams. The expected energy spectrum of the electrons at the interaction region is shown in Figure 5(a). For the  $e^+e^-$  mode the background simulation [8] showed that the amount of background expected per bunch crossing for the TESLA design is about  $10^5$   $e^+e^-$  pairs with a total energy of  $1.5 \cdot 10^5$  GeV and about 0.13 events of the type  $\gamma\gamma \rightarrow$  hadrons for hadronic masses  $W_{\text{had}} > 5$  GeV with an average visible energy of  $\langle E_{\text{vis}} \rangle = 10$  GeV, see Figure 5(b). The prospects of two photon physics measurements have to be discussed in the context of this expected machine parameter dependent 'soft' underlying background.

### 3 Some selected physics topics

The main processes that will be studied at a future linear collider are  $e^+e^-$  annihilation reactions. Figure 6 shows the cross sections for those reactions together with the cross sections for  $e^- \gamma$  and  $\gamma\gamma$  reactions as a function of the respective centre-of-mass energy [9]. The calculations are performed for a restricted range in polar angle,  $\theta$ , for the outgoing

particles or partons from the hard sub-process,  $10 < \theta < 170$  deg. In addition the invariant masses of the  $\mu^+\mu^-$  and  $q\bar{q}$  final states in the inelastic Compton processes are restricted to  $M_{\mu^+\mu^-,q\bar{q}} > 50$  GeV.

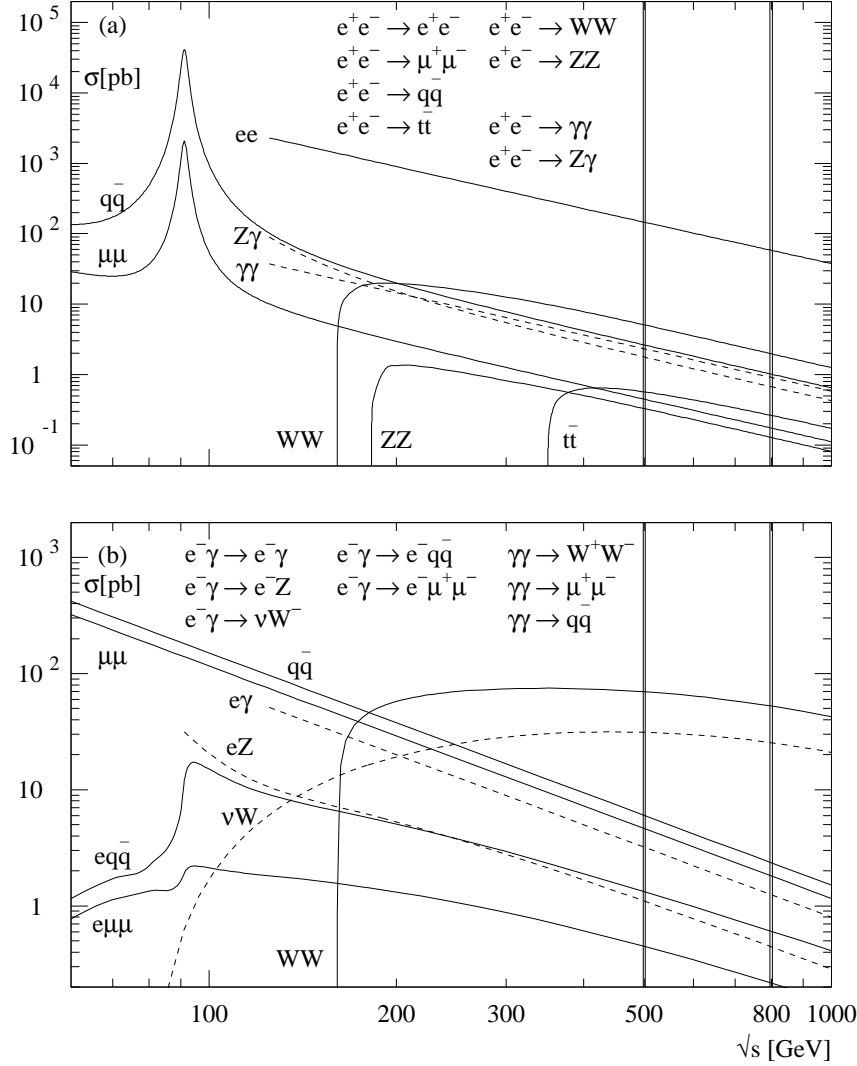


Figure 6: The expected cross sections as a function of the centre-of mass energies, from Ref. [9]. Shown are (a) some  $e^+e^-$  reactions and (b)  $e^- \gamma$  and  $\gamma\gamma$  reactions, all as functions of the respective centre-of mass energy  $\sqrt{s_{ee}}$ ,  $\sqrt{s_{e^- \gamma}}$  or  $\sqrt{s_{\gamma\gamma}}$ .

For an integrated luminosity of about  $20 \text{ fb}^{-1}$  per year of operation the expected event rate for a cross section of 1 pb is 20000 events. It can be seen that e.g. the available cross section for  $W$  production is much higher in the  $\gamma\gamma$  mode than in the  $e^+e^-$  mode at  $\sqrt{s_{ee}} = \sqrt{s_{\gamma\gamma}}$ . Given this it is clear that the scenario for two-photon physics will be very much depending on whether a PLC can be build or not.

The following topics will be discussed:

1. The total hadronic photon-photon cross section
2. Jet cross sections in photon-photon scattering
3. The measurement of the photon structure function  $F_2^\gamma$
4. The charm part  $F_{2,c}^\gamma$  of the structure function  $F_2^\gamma$
5. The signature of the BFKL Pomeron in  $\sigma_{\gamma^*\gamma^*}$

6. The production of  $W$  pairs
7. The Higgs discovery potential of the process  $\gamma\gamma \rightarrow H \rightarrow b\bar{b}$ , the total decay width  $\Gamma(H \rightarrow \gamma\gamma)$  and the reaction  $\gamma\gamma \rightarrow H \rightarrow ZZ$

Several topics are not covered, amongst those are e.g. resonances, searches for new particles other than the Higgs boson, diffraction, the production of photon pairs, and much more. The considerations for the selected topics are based on the energy spectrum of the bremsstrahlung photons using the equivalent photon approximation, EPA, on the energy spectrum of the beamstrahlungs photons which strongly depends on the machine parameters and on the energy spectrum of the Compton scattered photons for specific configurations of a PLC.

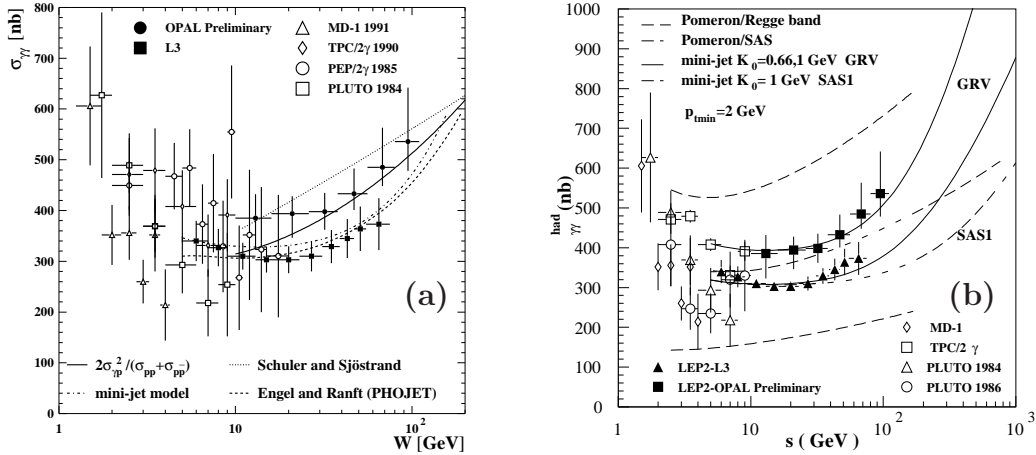


Figure 7: The total cross section measurements and theoretical expectations. Shown are (a) the LEP measurements together with the older data compared to several theoretical predictions, from Ref. [10], and (b) a comparison of the data with predictions from the eikonalised minijet model and Regge based models with extrapolations to higher energies, from Ref. [11].

The total hadronic cross section  $\sigma_{\gamma\gamma}$  for the reaction  $\gamma\gamma \rightarrow \text{hadrons}$  is of special theoretical interest as it allows to test theories which try to consistently describe proton-antiproton, proton-proton, photon-proton and photon-photon interactions [11, 12]. Only a slow rise as function of the photon-photon invariant mass is predicted for  $\sigma_{\gamma\gamma}$ , which means that a very large lever arm is needed in order to disentangle the different slopes of the various predictions. Compared to the pre LEP data there is already quite an improvement on precision and lever arm from the LEP data, see Figure 7, and indeed a slow rise is seen in the OPAL [10] and L3 [13] data. This measurement can be extended to larger values of  $W$  with a future linear collider, but it has to be kept in mind that the precision of the present LEP data is limited by the uncertainty of the theoretical description of the observable and especially also the unobservable hadronic final states as implemented in Monte Carlo models.

Looking more exclusively than the total cross section NLO jet cross sections can be confronted with the data. This has been done at LEP [14], Figure 8(a), and good agreement was found between the inclusive jet cross sections observed on the hadronic level and the NLO calculations of Ref. [15]. This measurement gives information on the relative amount of the direct processes, in which the photon directly takes part in the hard

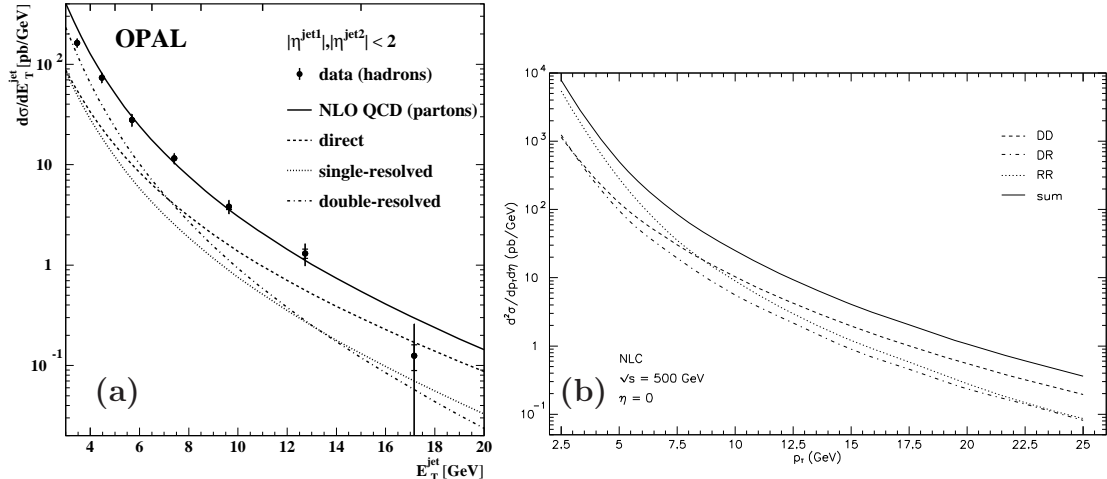


Figure 8: Measured inclusive jet cross sections [14] and the accessible range for a future linear collider. Shown are (a) the inclusive di-jet cross sections from OPAL compared to the NLO predictions of Ref. [15] and (b) the NLO predictions for a future linear collider, where D stands for direct and R for resolved.

interaction, and the resolved processes, where either one or both photons resolve into a partonic state and only one of the partons, either a quark or a gluon, takes part in the hard interaction. These measurements can be extended, Figure 8(b), to larger jet transverse momenta [15]. However it has to be kept in mind that in this region the jet cross section is dominated by direct processes where not much information on the internal structure of the photon can be obtained. This fact can be circumvented by using the di-jet sample and separating the direct and the resolved processes by measuring the fraction of the photon momentum,  $x_\gamma$ , which participates in the hard interaction [14]. Another important part is the region of low jet transverse momenta which is dominated by processes initiated by the gluons in the photon. Again this is a theoretically difficult region because the jet transverse momentum is the hard scale in the process which should not get too small in order for theoretical predictions to be reliable.

Structure function measurements are an active research project at LEP and the results cover the  $Q^2$  range from about 1.5 to 300 GeV<sup>2</sup> and the  $x$  range from 0.001 to about 1. Two main questions are addressed, the behaviour of the photon structure function  $F_2^\gamma$  at low values of  $x$  and the  $Q^2$  evolution of the structure function  $F_2^\gamma$  at medium  $x$ , see Ref. [16] for a review. Both these topics can be studied at a future linear collider but stringent requirements have to be imposed on the detector design [9]. The region of high  $Q^2$  and high  $x$  can already be studied with an electromagnetic calorimeter located outside the shielding mask covering polar angles of the tagged electrons of  $\theta_{tag} > 175$  mrad which is able to detect electrons with energies above 50% of the beam energy, Figure 9(a,b). The errors shown in Figure 9 are the quadratic sum of the statistical and the systematic components. The statistical error is calculated based on the GRV LO structure function  $F_2^\gamma$  [17] for an integrated luminosity of 10 fb<sup>-1</sup>. The systematic error is assumed to be equal to the statistical error but amounts to at least 5%. Therefore the precision indicated in Figure 9 has to be taken with care as the systematic errors shown do not reflect the present level of precision of the LEP data. In order to achieve overlap in  $Q^2$  with the LEP data the electron detection has to be possible down to  $\theta_{tag} > 40$  mrad, Figure 9(c,d),



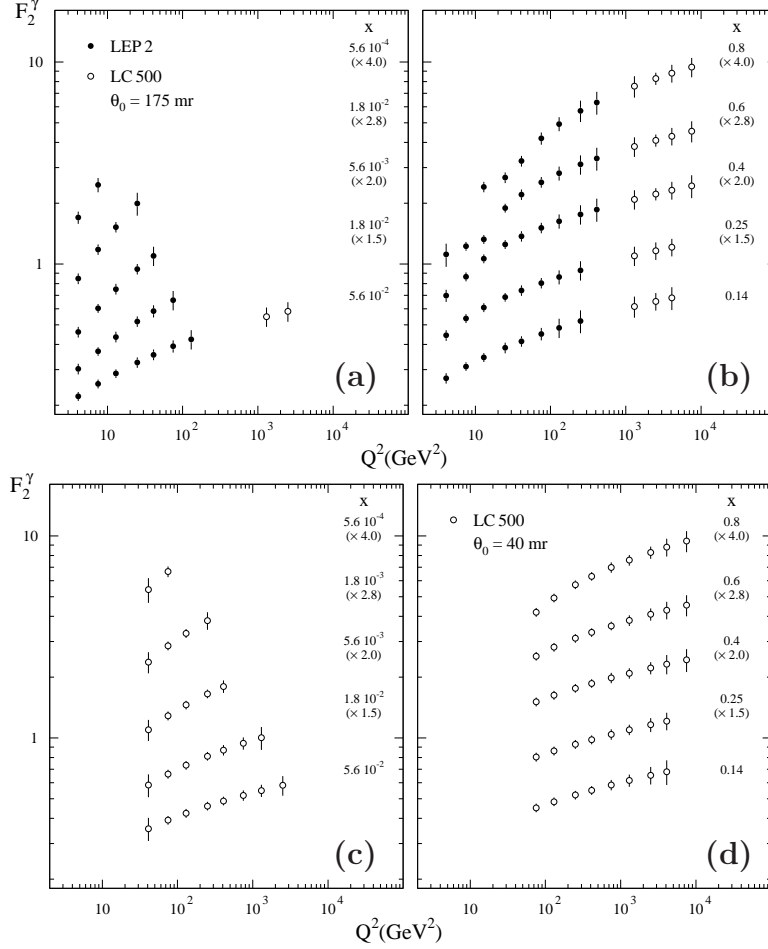


Figure 9: The prospects for structure function measurements at a future linear collider, from Ref. [9]. Shown are hypothetical LEP data and linear collider data for different minimal detection angles of the scattered electrons,  $\theta_{\text{tag}}$ . In (a,b)  $\theta_{\text{tag}} > 175$  mrad is assumed and (c,d) is based on  $\theta_{\text{tag}} > 40$  mrad.

which means the mask has to be instrumented, and the calorimeter has to be able to detect electrons which carry 50% of the beam energy in the huge but flat background of electron pairs discussed in Section 2.

The measurement of the  $Q^2$  evolution of the structure function  $F_2^\gamma$  constitutes a fundamental test of QCD. The status of the measurements as of today is reviewed in Figure 10, which is taken from Ref. [16] and extended by adding the preliminary measurement from L3 at  $Q^2 = 120$  GeV $^2$ , see Ref. [18]. The prospects of the extension of the measurement at a future linear collider with  $\sqrt{s} = 500$  GeV are shown for two scenarios. It is assumed that electrons can be tagged for energies  $E_{\text{tag}}/E_b > 0.5$  and for angles of  $\theta_{\text{tag}} > 40$  mrad (LC1) and  $\theta_{\text{tag}} > 175$  mrad (LC2). The measured values are taken to be equal to the prediction of the leading order GRV photon structure function  $F_2^\gamma$  in the respective ranges in  $x$ , which are chosen to be  $0.1 < x < 0.6$  for LC1 and  $0.3 < x < 0.8$  for LC2. The statistical errors of the hypothetical measurements are calculated from the number of events as predicted by the HERWIG Monte Carlo [19] for the leading order GRV photon structure function  $F_2^\gamma$  in bins of  $Q^2$  using the ranges in  $x$  as indicated in Figure 10. The systematic error is assumed to be 6.7% and to be independent of  $Q^2$ . This assumption is based on

the systematic error of the published LEP result with the highest  $Q^2$  from OPAL [20]. The symmetrised value of the published systematic error at  $Q^2 = 135 \text{ GeV}^2$  is 13.4%. It is assumed that this error can be improved by a factor of two. With this assumptions the error on the measurement is dominated by the systematic error up to the highest  $Q^2$  values. It is clear from Figure 10 that overlap in  $Q^2$  with the existing data can only be achieved if electron detection with  $\theta_{\text{tag}} > 40 \text{ mrad}$  is possible. For  $\theta_{\text{tag}} > 175 \text{ mrad}$  sufficient statistics is only available for  $Q^2$  above around  $1000 \text{ GeV}^2$ .

In summary with the data from the linear collider the measurement of the  $Q^2$  evolution of the structure function  $F_2^\gamma$ , Figure 10, can be extended to about  $Q^2 = 20000 \text{ GeV}^2$  and the behaviour of  $F_2^\gamma$  at low values of  $x$  can be investigated down to  $x \approx 5 \cdot 10^{-2}$  ( $x \approx 5 \cdot 10^{-4}$ ) for an electron acceptance of  $\theta_{\text{tag}} > 175 \text{ mrad}$  ( $\theta_{\text{tag}} > 40 \text{ mrad}$ ) [9].

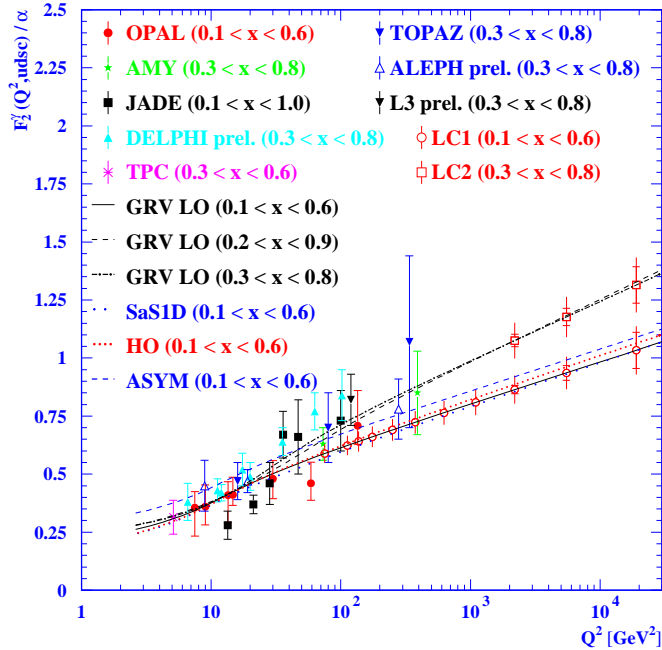


Figure 10: The measured  $Q^2$  evolution of  $F_2^\gamma$  from Ref. [16] extended by a preliminary measurement from L3 and by the prospects of a measurement at a future linear collider.

For a PLC a completely new scenario for photon structure function measurements would be opened. For the first time measurements could be performed with beams of high energetic photons of known energy with a rather small energy spread instead of measurements using the broad bremsstrahlungs spectrum of photons radiated by electrons. With this the measurements of the photon structure function would be on a similar ground than the measurement of the proton structure function at HERA. Another very important improvement for structure function measurements would be the detection of the electron that radiates the quasi-real photon and is scattered under almost zero angle. If this could be achieved the precision of structure function measurements would significantly be improved, because  $x$  could be calculated from the two detected electrons, and therefore independently of the hadronic final state. Given that the dominant systematic error of the structure function measurement comes from the imperfect description of the hadronic

final state by the Monte Carlo models, this would be an important step to reduce the systematic error of structure function measurements.

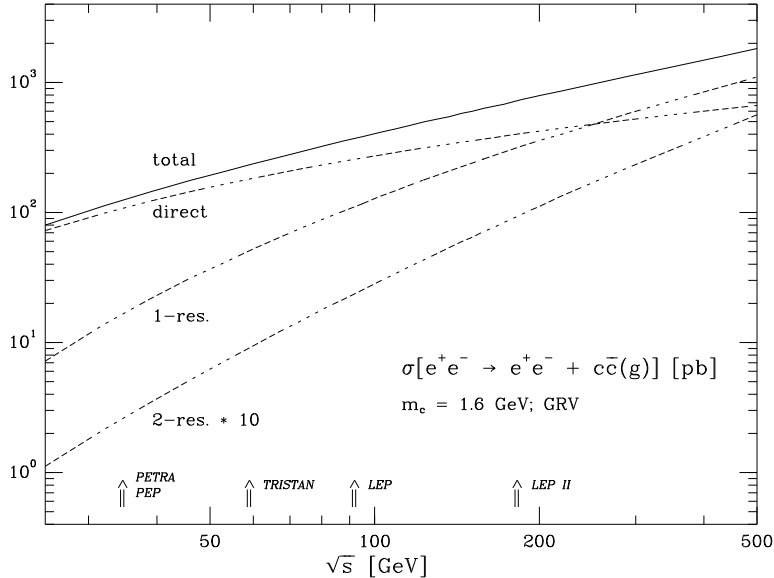


Figure 11: The charm cross section for photon-photon interactions, from Ref. [21]. Shown are the total cross section (full line) and the individual contributions, direct (direct), single resolved (1-res) and double resolved (2-res).

Pairs of charm quarks will be copiously produced at a future linear collider. Figure 11 shows the calculation from Ref. [21] for the production of  $c\bar{c}$  pairs in photon-photon scattering based on the bremsstrahlung photons approximated by the EPA. The prediction is about  $4 \cdot 10^7$   $c\bar{c}$  events with  $W_{\min} = 3.8$  GeV for an integrated luminosity of  $20 \text{ fb}^{-1}$ . This calculation takes into account the direct and the single-resolved contribution in NLO, and the double-resolved contribution, which is much smaller, in LO. The mass of the charm quark is taken to be  $m_c = 1.6$  GeV, the renormalisation scale is set to  $\mu = \sqrt{2}m_c$  and  $\Lambda^{(4)} = 340$  MeV in the  $\overline{\text{MS}}$  scheme. The cross section of the direct process is a pure QCD prediction which only depends on the mass of the charm quark and on  $\alpha_s$ . It has been shown [22] that a fair amount of these events can be observed within the acceptance of the detector allowing to test this pure QCD prediction.

Also in the case of deep inelastic electron-photon scattering charm quark pairs are frequently produced [23]. The contribution of the individual quark species to the structure function  $F_2^\gamma$  is proportional to the quark charge squared, which means that at high invariant masses the charm contribution to  $F_2^\gamma$  should be almost as large as the contribution from up quarks. Due to the low efficiency for charm tagging the charm quark contribution to  $F_2^\gamma$  has never been measured. The structure function  $F_{2,c}^\gamma$  receives two contributions which are clearly separated in  $x$ , Figure 12. At low values of  $x$  the hadronic contribution dominates, whereas the point-like contribution is concentrated at high values of  $x$ . The NLO corrections are rather small, see Figure 12, indicating a good stability of the perturbative QCD prediction. The hadronic contribution is directly proportional to the gluon density in the photon and due to the large mass of the charm quark the point-like contribution is a pure QCD prediction which is unambiguously defined to NLO [23]. Given this a simultaneous measurement of the gluon density in the photon and of a pure QCD

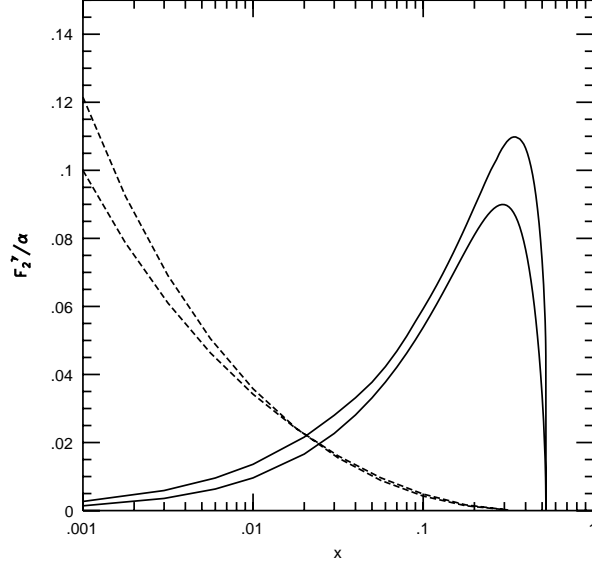


Figure 12: The expected charm contribution to  $F_2^\gamma$  at  $Q^2 = 10 \text{ GeV}^2$  in LO and NLO, from Ref. [23]. The dashed lines denote the hadronic and the full lines the point-like contributions to  $F_{2,c}^\gamma$ . The lower solid line is the LO and the upper solid line the NLO prediction. At  $x = 0.001$  the lower dashed line is the NLO and the upper dashed line is the LO prediction.

prediction is possible using the production of charm quark pairs in deep inelastic electron-photon scattering. The calculations from Ref. [23] show that for  $E_{\text{tag}}/E_b > 0.5$ ,  $\theta_{\text{tag}} > 40 \text{ mrad}$ ,  $m_c = 1.5 \text{ GeV}$ ,  $\mu = Q$  and a charm tagging efficiency of 1-2% several thousand events could be seen for an integrated luminosity of  $20 \text{ fb}^{-1}$ . A good understanding of the spectrum of beamstrahlungs photons is needed as they contribute a significant fraction to the production of the charm quark pairs.

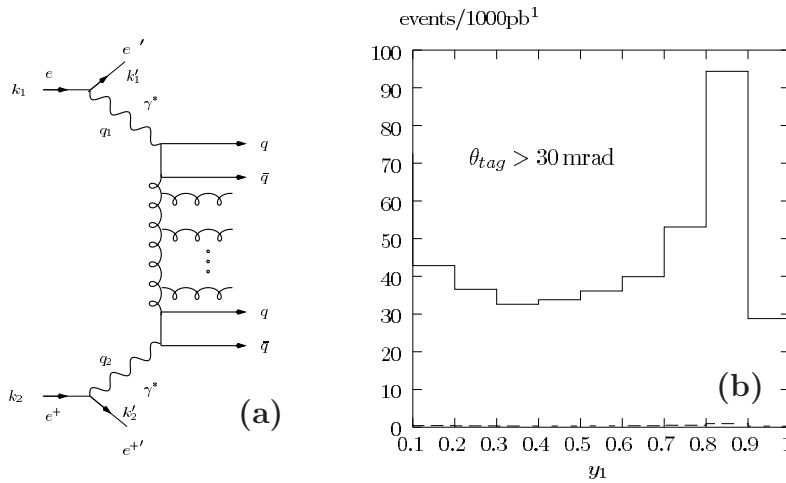


Figure 13: The signature of the BFKL Pomeron in  $\sigma_{\gamma^* \gamma^*}$ , from Ref. [25]. Shown are (a) a sketch of the process and (b) the expected event rates with (full line), and without (dashed line) the BFKL Pomeron for a specific phase space, see text.

Since quite some time the search of BFKL signatures at HERA attracted broad interest. The observables studied are the behaviour of the proton structure function at small values of  $x$  and the production of forward jets. In  $e^+e^-$  collisions the BFKL Pomeron would show up in an enhanced total cross section for the scattering of highly virtual photons,  $\sigma_{\gamma^*\gamma^*}$  [24–26]. The diagram of the reaction is shown in Figure 13(a). In order to freeze the  $Q^2$  evolution the two photons are required to have similar virtualities. Then the BFKL Pomeron would lead to an enhanced cross section over the two gluon exchange, which is the first significant contribution without BFKL. Defining,  $y_1 = q_2 k_1 / k_1 k_2$ ,  $y_2 = q_1 k_2 / k_1 k_2$ ,  $Q_i^2 = -q_i^2$ ,  $s = (k_1 + k_2)^2$  and  $s_0 = \sqrt{Q_1^2 Q_2^2 / y_1 y_2}$  the cross section expected for the kinematical range,  $\theta_{\text{tag}} > 30$  mrad,  $E_{\text{tag}} > 20$  GeV,  $\log(s/s_0) > 2$  and  $2.5 < Q_i^2 < 200$  GeV<sup>2</sup> is about 0.3 pb. This means a yield of  $\mathcal{O}(6000)$  events for an integrated luminosity of  $20 \text{ fb}^{-1}$  with practically no background from the two gluon exchange process, see Figure 13(b). The detector requirements are very demanding. In order to observe the BFKL signal which dies out like  $Q^{-6}$  the instrumentation of the mask is a must. In addition the observation of the enhancement relies on the ability to detect electrons of relatively low energy of only 20 GeV. This is very challenging given the magnitude of the expected machine background discussed above.

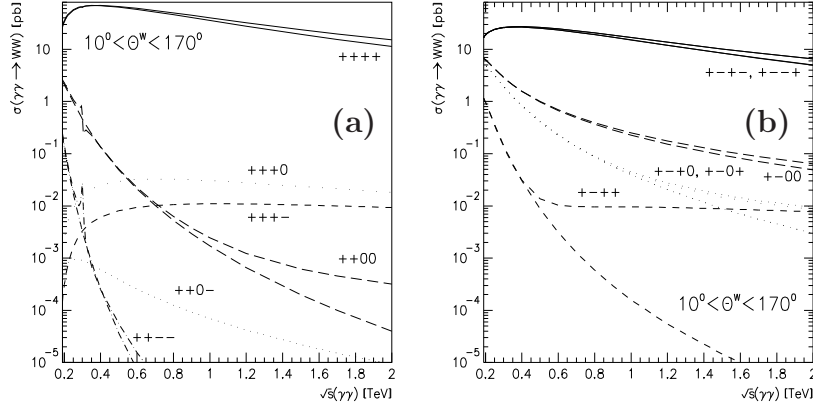


Figure 14: The prospects for  $W$  pair production at a future linear collider, from Ref. [27]. Shown are the Born cross sections and the  $\mathcal{O}(\alpha)$  cross sections for the reaction  $\gamma\gamma \rightarrow W^+W^-(\gamma)$  for different helicity states of the incoming photons and the outgoing  $W$  bosons. The curves nearest to the helicity symbols denote the  $\mathcal{O}(\alpha)$  corrected cross sections.

Due to the high energy photons produced at a PLC the large cross section for  $\gamma\gamma \rightarrow W^+W^-(\gamma)$  can be exploited. Figure 14 shows the cross sections for  $WW$  and  $WW\gamma$  final states for the Born term and the  $\mathcal{O}(\alpha)$  corrections in a restricted range in polar angle of the  $W$  bosons,  $10 < \theta^W < 170$  deg, [27]. The cross section at  $\sqrt{s_{\gamma\gamma}} = 500$  GeV within this restricted range is  $\sigma_{\gamma\gamma} = 61$  pb, which is to be compared with a cross section of only  $\sigma_{ee} = 6.6$  pb in the  $e^+e^-$  case at  $\sqrt{s_{ee}} = 500$  GeV. It is found that the radiative corrections are moderate at  $\sqrt{s_{\gamma\gamma}} = 500$  GeV but do strongly depend on  $\theta^W$ , so special care has to be taken. With such a sample of  $\mathcal{O}(10^6)$   $W^+W^-$  pairs per year detailed studies of the anomalous couplings of the  $W$  can be performed. With the natural order of magnitude of the predicted anomalous couplings the standard model cross sections have to be known to better than 1% to measure these small numbers. Given the high rate and

the precise prediction the  $W$  pair production is in addition a good candidate to monitor the  $\gamma\gamma$  luminosity at a PLC.

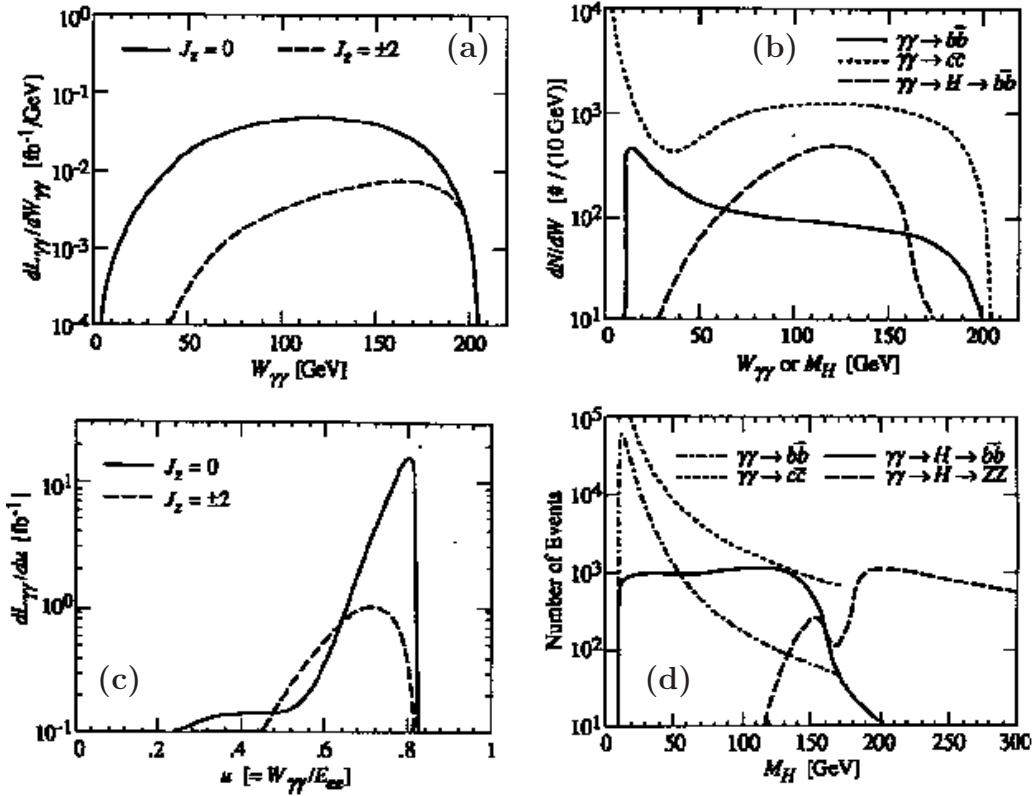


Figure 15: Higgs production at a future linear collider, from Ref. [28]. Shown are (a) the photon luminosity spectrum assumed for the Higgs search, (b) the expected event rate using the spectrum of (a), (c) the photon luminosity spectrum assumed for the measurement of  $\Gamma(H \rightarrow \gamma\gamma)$  and (d) the expected event rate for the measurement of  $\Gamma(H \rightarrow \gamma\gamma)$  using the spectrum of (c).

Since long the search for the Higgs boson has been performed at various colliders, but without success so far. The PLC collider is an ideal place to search for the Higgs boson as at such a machine the Higgs boson is produced as an s-channel resonance. The most promising channel is  $\gamma\gamma \rightarrow H \rightarrow b\bar{b}$ . This channel receives background from the non resonant production of  $b\bar{b}$  pairs and also of  $c\bar{c}$  pairs which are misidentified as  $b\bar{b}$  final states. To achieve a good signal to noise ratio several facts have to be exploited [28]. To suppress the continuum production of  $b\bar{b}$  and  $c\bar{c}$  a vanishing third component of the total angular momentum of the  $\gamma\gamma$  system,  $J_z = 0$ , Figure 15(a), has to be selected. In addition a good tagging efficiency for bottom quarks,  $\epsilon_b > 90\%$ , and a good suppression of charm quarks of  $\epsilon_{c \rightarrow b} < 5\%$  is mandatory. Assuming these numbers, together with a mass resolution of  $0.1M_H$  (FWHM), a signal with larger than  $10\sigma$  significance can be established in the range  $80 < M_H < 140$  GeV for an integrated luminosity of  $10 \text{ fb}^{-1}$  [28], Figure 15(b). Once the Higgs has been seen a very fundamental measurement to be performed is the determination of the total width,  $\Gamma(H \rightarrow \gamma\gamma)$ , as it is sensitive to all new particles in the loop which couple to the Higgs. The results of a feasibility study [28] can be seen in Figure 15(c,d), where the expected event rates are calculated for a restricted range in polar angle for the produced Higgs bosons of  $|\cos\theta| < 0.7$ . Assuming a resolution

of  $\sigma_{M_H} = 0.1M_H$  the total width  $\Gamma(H \rightarrow \gamma\gamma)$  can be determined with an  $\mathcal{O}(10\%)$  error for an integrated luminosity of  $10 \text{ fb}^{-1}$  [28].

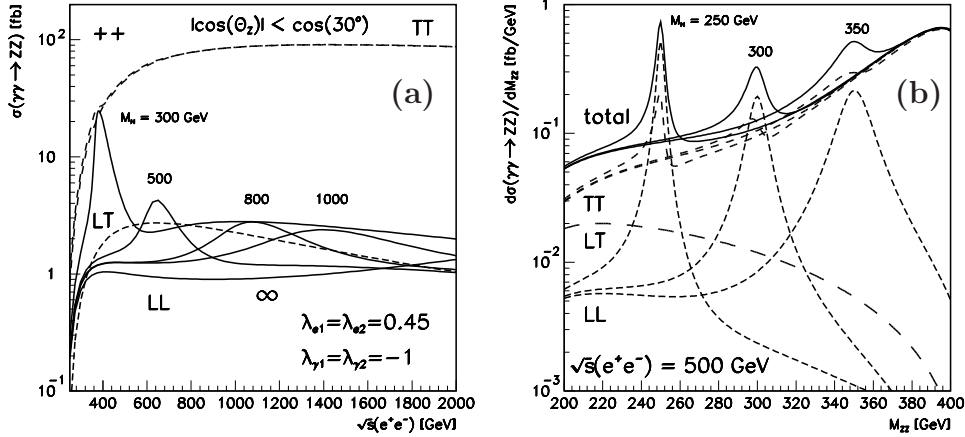


Figure 16: Prospects for the Higgs search in the reaction  $\gamma\gamma \rightarrow H \rightarrow ZZ$ , from Ref. [29]. Shown are (a) the cross sections as a function of the  $e^+e^-$  centre-of-mass energy and (b) the invariant mass distributions at  $\sqrt{s_{ee}} = 500 \text{ GeV}$  for  $Z$  pair production in  $\gamma\gamma$  collisions at a future linear collider using the photon spectrum of a PLC. The curves are for different helicities of the  $Z$  bosons and different masses of a hypothetical Higgs boson.

Another interesting channel is the reaction  $\gamma\gamma \rightarrow H \rightarrow ZZ$ . As can be seen from Figure 16 the cross section strongly depends on the helicities of the  $Z$  bosons. In this channel Higgs signals up to  $M_H = 350 \text{ GeV}$  can be observed. For higher masses the background from the continuum  $Z_T Z_T$  production is too high [29].

## 4 Summary

The linear collider is an unique place to investigate two photon physics at the highest energies. Due to the high centre-of-mass energy of the photon-photon system especially in the case of the  $\gamma\gamma$  collider new channels like Higgs bosons,  $W$  pairs and  $Z$  pairs are open to be copiously produced in reactions of two photons. This opens a very rich field of interesting measurements to be performed. The tagging of electrons down to the lowest possible angles is a challenging task, but it is mandatory in order to achieve overlap in  $Q^2$  with the measurements of the photon structure function  $F_2^\gamma$  at LEP. In this report the available information on the prospects for the measurement of the structure function  $F_2^\gamma$  at a future linear collider was extended by a detailed discussion of the prospects for the measurement of the  $Q^2$  evolution of  $F_2^\gamma$ . In all physics channels a careful determination of the  $\gamma\gamma$ ,  $e\gamma$  and  $ee$  luminosity distributions is essential. Lots of work is in front of us to bring a linear collider to life, but it should be fun and the physics potential is certainly worth the effort.

## Acknowledgements

I wish to thank Albert De Roeck for useful discussions and Bernd Surrow for presenting the results on my behalf at the conference.

## References

- [1] I. F. Ginzburg, G. L. Kotkin, V. G. Serbo, and V. I. Telnov, Nucl. Instr. and Meth. **205**, 47–68 (1983);  
I. F. Ginzburg et al., Nucl. Instr. and Meth. **219**, 5–24 (1984);  
V. Telnov, Nucl. Instr. and Meth. **A294**, 72–92 (1990);  
V. Telnov, Nucl. Instr. and Meth. **A355**, 3–18 (1995).
- [2] R. Bossart et al., CLIC, a 0.5 to 5 TeV  $e^+e^-$  Compact Linear Collider, CERN/PS/98-009 (1998).
- [3] N. Akasaka et al., JLC design study, KEK-REPORT-97-1 (1997).
- [4] C. Adolphsen et al., Zeroth-order design report for the Next Linear Collider, SLAC-474 (1996).
- [5] R. Brinkmann et al., Conceptual Design Report of a 500 GeV  $e^+e^-$  Linear Collider with Integrated X-ray Laser Facility, (1997).
- [6] V. Telnov, High-energy photon-photon colliders, BUDKERINP-97-71, 18pp (1997), physics/9710014.
- [7] V. Telnov, Int. J. Mod. Phys. **A13**, 2399–2410 (1998).
- [8] D. Schulte, Study of electromagnetic and hadronic background in the interaction region of the TESLA collider, DESY-TESLA-97-08, 171pp (1997).
- [9] E. Accomando et al., Phys. Rept. **299**, 1–78 (1998).
- [10] F. Wackerle, Total hadronic cross-section for photon-photon interactions at LEP, in *Proceedings of the 27th International Symposium on Multiparticle Dynamics, Frascati*, page 7, World Scientific, 1997, hep-ex/9710005.
- [11] A. Corsetti, R. M. Godbole, and G. Pancheri, Phys. Lett. **B435**, 441–448 (1998).
- [12] A. Donnachie and P. V. Landshoff, Phys. Lett. **B296**, 227–232 (1992);  
G. A. Schuler and T. Sjöstrand, Z. Phys. **C73**, 677–688 (1997);  
R. Engel, Z. Phys. **C66**, 203–214 (1995);  
R. Engel and J. Ranft, Phys. Rev. **D54**, 4244–4262 (1996).
- [13] M. Acciarri et al., Phys. Lett. **B408**, 450–464 (1997), L3 Collaboration.
- [14] G. Abbiendi et al., submitted to Eur. Phys. J. **C** (1998), OPAL Collaboration CERN-EP/98-113.
- [15] T. Kleinwort and G. Kramer, Nucl. Phys. **B477**, 3–26 (1996).



- [16] R. Nisius, The photon structure function measurements from LEP, in *Proceedings of the International Europhysics Conference on High Energy Physics 97, Jerusalem, 1997*, hep-ex/9712012, to be published.
- [17] M. Glück, E. Reya, and A. Vogt, Phys. Rev. **D45**, 3986–3994 (1992);  
M. Glück, E. Reya, and A. Vogt, Phys. Rev. **D46**, 1973–1979 (1992).
- [18] R. Freudenreich, Photon Structure Functions at LEP, in *Proceedings of ICHEP'98, Vancouver, Canada, July 22-30, 1998*, World Scientific, 1998, to be published.
- [19] G. Marchesini and B. R. Webber, Nucl. Phys. **B310**, 461–526 (1988);  
I. G. Knowles, Nucl. Phys. **B310**, 571–588 (1988);  
S. Catani, G. Marchesini, and B. R. Webber, Nucl. Phys. **B349**, 635–654 (1991);  
G. Abbiendi and L. Stanco, Comp. Phys. Comm. **66**, 16–24 (1991);  
M. H. Seymour, Z. Phys. **C56**, 161–170 (1992).
- [20] K. Ackerstaff et al., Phys. Lett. **B411**, 387–401 (1997), OPAL Collaboration.
- [21] M. Drees, M. Krämer, J. Zunft, and P. M. Zerwas, Phys. Lett. **B306**, 371–378 (1993).
- [22] M. Cacciari et al., Nucl. Phys. **B466**, 173–188 (1996).
- [23] E. Laenen and S. Riemersma, Phys. Lett. **B376**, 169–176 (1996).
- [24] J. Bartels, A. De Roeck, and H. Lotter, Phys. Lett. **B389**, 742–748 (1996).
- [25] J. Bartels, A. De Roeck, C. Ewerz, and H. Lotter, The  $\gamma^*\gamma^*$  total cross-section and the BFKL pomeron at the 500 GeV  $e^+e^-$  linear collider, (1997), hep-ph/9710500.
- [26] S. Brodsky, F. Hautmann, and D. E. Soper, Phys. Rev. **D56**, 6957–6979 (1997);  
S. Brodsky, F. Hautmann, and D. E. Soper, Phys. Rev. Lett. **78**, 803–806, Erratum–  
ibid **79** 3544 (1997).
- [27] G. Jikia, Nucl. Phys. **B494**, 19–40 (1997).
- [28] D. L. Borden, D. A. Bauer, and D. O. Caldwell, Phys. Rev. **D48**, 4018–4028 (1993).
- [29] G. Jikia, Turk. J. Phys. **22**, 705–713 (1998).